DEVELOPMENT AND CHARACTERIZATION OF IN-SITU AA2024-Al_3NiCu COMPOSITES

Ramezanali Farajollahi, Hamed Jamshidi Aval and Roohollah Jamaati
Department of Materials Engineering, Babol Noshirvani University of Technology, Shariati Avenue, Babol 47148-71167, Iran

https://doi.org/10.1007/s40962-021-00752-y

Abstract

This research aims to study the effect of nickel additive and heat treatment effects on microstructure and mechanical properties of in-situ AA2024-Al_3NiCu composite fabricated by the stir casting method. The effects of artificial aging heat treatment, after the homogenization of as-cast composites, were investigated in this study. The results indicated that, after artificial aging, the precipitate-free zone at the inter-dendritic zone disappeared or became smaller. With the addition of nickel up to 3 wt% as well as the aging process, S-Al_2CuMg precipitates will be reduced and their size will be smaller. However, after adding 4.5 wt% of nickel and, also, performing aging heat treatment, it is not possible to precipitate the S- Al_2CuMg precipitates, and, instead of it, the T-Al_6CuMg_4 precipitates will be formed. By increasing the nickel amount from 3 to 4.5 wt%, the hardness, ultimate tensile strength, and toughness, after aging treatment, decreases 8, 19, and 28 %, respectively. By adding nickel and performing aging treatment at 200 °C for 120 min, the maximum hardness, ultimate tensile strength, and toughness achieved in the 3 wt% nickel-containing sample as 134.10 ± 4.89 HV, 251.23 ± 3.70 MPa, and 1.96 ± 0.09 MJ.$m^{-3,}$ respectively. The hardness, ultimate tensile strength, and toughness of AA2024-Al_3NiCu composite, after aging treatment, increased 11, 49, and 139%, respectively, compared to nickel-free AA2024 aluminum alloy matrix.

Keywords: *in-situ AA2024-Al_3NiCu composite, stir casting, nickel additive, aging treatment*

Introduction

Development in industries, such as automobiles and aerospace, depends on the continuous development of aluminum alloys for better mechanical performance. In addition, the goal is to reduce construction costs, but maintain high strength in components.[1] Aluminum matrix composites (AMCs) are one of the most important engineering materials in the present age.[2] These materials are increasingly preferred and used in various applications in the aerospace, automotive, and marine industries. The reason for using these composites in these industries can be attributed to the high strength-to-weight ratio at room and high temperatures, excellent fatigue properties, and improved wear properties compared to conventional aluminum alloys.[3,4] Among the many methods for making particle-reinforced AMCs, due to the simplicity of the process, the stir casting process is known as a desirable and cost-effective method.[5] The properties of the AMCs can be improved by the correct selection of reinforcing materials. The size, volume fraction, and types of reinforcement affect the mechanical properties and wear properties of AMC.[6] In the ceramic reinforced AMCs, the poor wettability between ceramic particles and the aluminum matrix is problematic.[7,8] This problem can be, somewhat, overcome by coating the ceramic particles with a metal.[9] However, the formation of brittle reactive products at the interface between the reinforcement and the matrix weakens the mechanical properties of the composite.[10] Another solution to this problem is to use in-situ processes to create reinforcement in the aluminum matrix.[11–14]

Nickel is one of the metal particles used as reinforcement in the fabrication of AMCs. The better wettability of nickel, compared to ceramic particles, has made it a strong candidate for the reinforcing phase in the fabrication of AMCs to improve the strength, hardness, and toughness.[15] Nickel has little solubility in aluminum and does not form a supersaturated solid solution even during rapid cooling of the melt.

Received: 01 October 2021 / Accepted: 27 December 2021 / Published online: 31 January 2022

Nickel also forms the hard Al-Ni intermetallic compounds (IMCs) in the aluminum matrix.[16] Al-Ni IMCs have the characteristics of high-temperature strength, heat resistance, high thermal conductivity, and good corrosion resistance, which have led to their uses in the automotive industry, aerospace engineering, and power plants.[17] In addition, nickel in combination with copper improves strength and hardness at high temperatures.[18] Various studies have been performed on the fabrication of AMCs reinforced with nickel-aluminide compounds. The previous research by authors[19] found that the nickel aluminide reinforcement decreased the coefficient of friction and wear rate of the AA2024-Al_3NiCu composite. Also, it is reported that by increasing nickel from 3 to 4.5 wt%, in the homogenized composite, instead of S-Al_2CuMg precipitates, the T-Al_6Mg_4Cu precipitates formed. Najarian et al.[20] used 99.5% purity aluminum as a matrix and nickel oxide powder as a reinforcement in composite fabrication by stir casting technique. They found that mechanical properties of composites, such as ultimate tensile strength (UTS) and hardness, due to the dispersion of reinforcing particles in the aluminum matrix, have been improved. Ramesh et al.[21] fabricated an AA1100-Al_3Ni in-situ composite using the stir and squeeze casting methods. They also argued that increased amounts of Al_3Ni led to an improvement in the mechanical and tribological properties of the composite. It was also demonstrated that squeeze cast composites have better properties than stir cast composites. Liu et al.[4] found that the addition of nickel to the Al-Zn-Mg-Cu alloy, produced by gravity casting, increases the Al_3Ni phase fraction, but it has no effect on the formation of the η-$MgZn_2$ and S-Al_2CuMg precipitates. Xuejian et al.[22] found that the addition of nickel to the Al-Li-Cu-Mg alloy, fabricated by the gravity casting process, changes the shape of grains. In addition, with increasing nickel content, nickel-rich precipitates change from discontinuous to continuous after aging treatment.

As mentioned, among all the manufacturing processes available for AMC fabrication, stir casting is a more economical technique that can produce pieces in large quantities.[23] In this research, the effect of nickel weight percentage and aging heat treatment on AA2024 composite, reinforced with Al-Ni IMCs, has been investigated and results after aging treatment, compared with results of as-cast and homogenized composite, reported previously at.[19] To produce this composite by stir casting process, nickel powder was injected into the melt by argon gas during stirring, and due to the chemical reaction between aluminum and nickel powder, the Al-Ni IMCs were formed in-situ.

Experimental Work

Materials and Stir Casting Process

To make AA2024 aluminum alloy matrix composite reinforced with in-situ nickel-aluminide, the AA2024 aluminum alloy with the chemical composition 0.14% Si, 0.26% Fe, 4.14% Cu, 0.49% Mn, 1.45% Mg, and Al balance (all in wt%) used as matrix. As shown in Figure 1, the 99.9% purity nickel powder with an approximate size of 20–70 μm was used as reinforcement. Nickel powder was added to the aluminum melt using a stir casting process. As shown schematically in Figure 2, various equipment, such as the resistive electric furnace, graphite crucible, electric motor for stirring the melt, steel stirrer coated with alumina, thermocouple, and reinforcement powder injection system, was used. The composite fabrication process begins with preheating the crucible in a resistive electric furnace. AA2024 aluminum alloy ingots are placed in the crucible. Hexachloroethane (C_2Cl_6) tablets are used for degassing the molten aluminum and the slag is removed. The stirrer is, then, introduced into the melt and the stirring operation is started by an electric motor equipped with a speed adjustment system. At this stage, first argon gas is introduced into the furnace atmosphere with a pressure of 3.5 bar, then nickel powder is introduced by inlet argon gas pressure 3.5 bar into the melt, and is distributed in the melt by rotation of stirrer. After complete injection of nickel powder, the melt stirring operation continues for 2 minutes to ensure both the reaction between the nickel/aluminum alloy and better distribution of nickel powder in the melt. Finally, the crucible is taken out of the furnace and molten materials poured into a sand mold to solidify completely. Bentonite is used as a binder in mold fabrication. To investigate the effect of nickel and aging heat treatment on the microstructure and mechanical properties of this composite, the composite fabrication process was performed with nickel percentages of 0%, 1.5%, 3%, and 4.5 wt%, and then homogenizing and aging treatment was performed on them. The stirring was performed for 20 minutes at a stirring speed of 450 rpm and a temperature of 750°C. It should be noted that each series of an experiment is repeated two times. As reported in Table 1, the stirring time,

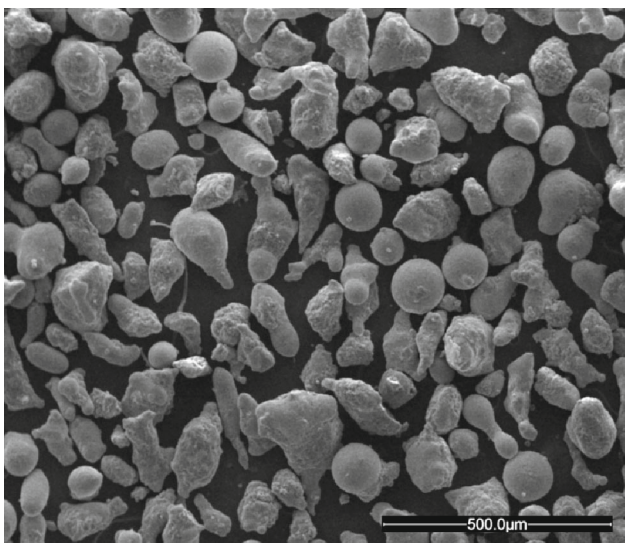

Figure 1. SEM micrographs of Ni powder.

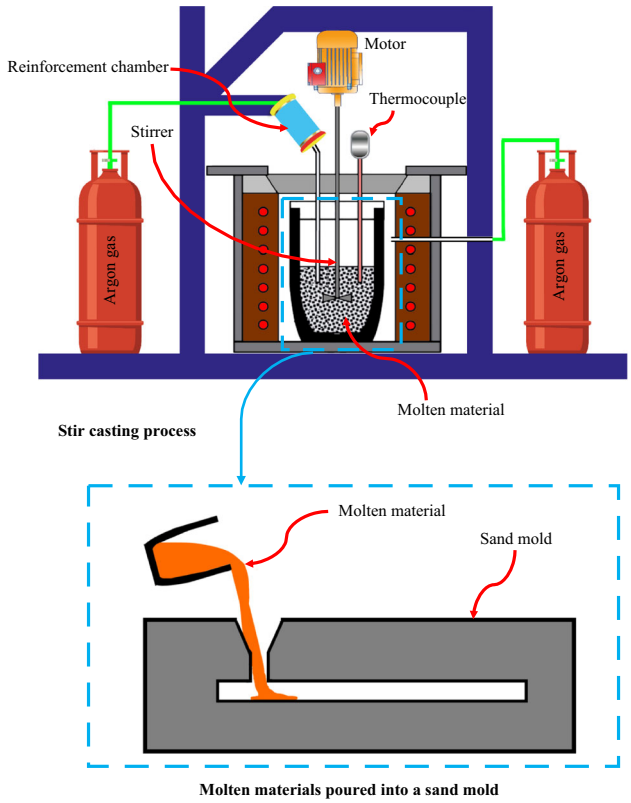

Figure 2. Schematic view of stir casting procedure.

stirring speed, and stirring temperature chosen by the preliminary study on the effect of casting parameters on the microstructure and mechanical properties of the composite at melting temperatures of 750 and 850°C, stirring times of 10 and 20 min, and stirring speeds of 300 and 450 rpm. Samples with zero, 1.5, 3, and 4.5 wt% nickel were named S-0, S-1.5, S-3, and S-4.5, respectively. For the aging heat treatment, the first, homogenized samples were solutionized at 505°C for 140 min and after quenching in the water, aged at 200 °C for 120 min. The homogenization heat treatment was performed at 500 °C for 24 hours on all samples. The aging and homogenizing treatment temperature and time were chosen according to a preliminary study by authors and the best temperature-time reported in the[24] to achieve maximum mechanical properties.

Table 1. The parameters and levels considered in the preliminary study of composite manufacturing.

Parameters	Levels
Stirring temperature, (°C)	750, 850
Stirring time, (min)	10, 20
Stirring speed (rpm)	350, 450

Microstructure Characterization

After cooling the melt, the as-cast rod (as shown in Figure 3) was used to extract metallographic and tensile test samples. Metallographic samples were taken from the rod's center. After cutting metallographic samples from the middle of cast pieces, for microstructural investigation, grinding of metallography sample cross-section is done with silicon carbide sandpaper, and then the samples are polished using alumina solution and, finally, etched with Keller's solution (2.5 ml nitric acid, 1.5 ml hydrochloric acid, and 1ml hydrofluoric acid) to reveal the microstructure. Microstructural images were taken from the cross-section of homogenized and aged samples by light and scanning electron microscopy (FEI ESEM QUANTA 200) equipped with the energy-dispersive X-ray spectroscopy (EDS) analysis. In addition, X-ray diffraction (XRD) analysis by XRD Philips PW1730 was performed to identify the compounds and phases in the samples. The porosity of the resulting composite was calculated using the following formula[25]:

$$\text{Porosity} = (1 - (\rho_s / \rho_{th})) \times 100 \qquad \text{Eqn. 1}$$

where ρ_s and ρ_{th} denote the composite density and the theoretical value of the porosity-free density, respectively, as determined by Archimedes' principle[26] and the mixtures rule.

Mechanical Tests

The Vickers hardness of the composites was determined using a Koopa Universal (UV1) testing machine according to ASTM E92 standard and by applying 15 kg of force and 10s of time, and averaging at least 15 indentations. Tensile test specimens were prepared with 24-mm gauge length and 6-mm diameter, according to Figure 4. The tensile test of the samples was conducted according to ASTM E8 at room temperature (25°C) by SANTAM STM 250 machine with a constant crosshead speed of 0.5 mm/min and three repeat times to determine the mechanical properties. The

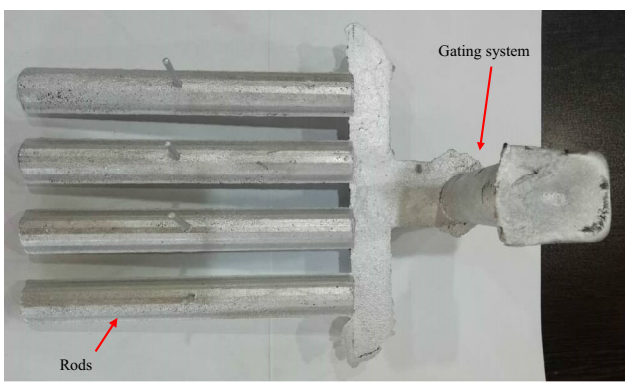

Figure 3. The as-cast rod.

toughness is calculated by using the area underneath the stress-strain curve.

Results and Discussion

Microstructure Analysis of Composites

Figure 5 shows the optical microscopy images of microstructures of different samples, both after homogenization and artificially aging treatment. Also, Figure 6 shows the porosity formed in the microstructure of different as-cast samples. As we can see, the microstructures include various inter-dendritic IMCs and fine precipitates scattered throughout the microstructure. In all artificially aged samples, the precipitates became finer and more uniform than that in the homogenized samples. In the inter-dendritic zone of homogenized samples, a precipitate-free zone formed. While after artificial aging, the precipitate-free zone disappeared or become smaller. Also, in the nickel-containing samples, the precipitates are finer than in nickel-free ones. It should be considered that with the increasing percentage of nickel in both homogenized and aged states, up to 3 wt% of nickel, the amount of precipitates in the microstructure decreases and increases again with increasing the percentage of nickel from 3 to 4.5 wt%. On the other hand, it is observed that, by adding nickel, a gray block phase is formed next to the dark phase and its amount is increased with increasing the percentage of nickel. These dark and gray phases are mainly formed in the inter-dendritic zone. It should also be noted that the second phase particles (appearing in black and gray in the microstructure) grow after the aging heat treatment.

To more accurately study the microstructure, understand the nature of the precipitates, and IMCs present on it, SEM examination was performed on different samples and the corresponding results are shown in Figure 7. In addition, EDS results of precipitates and IMCs are shown in Figure 8 and Table 2. The microstructure of sample S-0, in both homogenized and the aged state, contains S-Al_2CuMg, Al_7Cu_2Fe, and Al (Cu, Mn, Fe, Si) precipitates, and second phase particles. The fine black precipitates near the inter-dendritic zone are S-Al_2CuMg. By comparing results reported in the ref.[19] after the aging heat treatment, these precipitates become finer and uniformly distributed throughout the microstructure. The inter-dendritic zone is also surrounded by Al_7Cu_2Fe and Al (Cu, Mn, Fe, Si), second phase particles. Since the dissolution temperature of these intermetallic compounds is much higher than the homogenization and aging temperature, it is not possible to dissolve these compounds in the microstructure. The Si-rich particles, reported by other researchers in AA2024 aluminum alloy, are found in both homogenized and aged samples. Figure 7(b) shows the microstructure of the sample S-1.5 after aging treatment, respectively. As can be seen, by adding nickel, the Al_3NiCu and Al_9NiFe IMCs are formed in the microstructure. The formation of these IMCs, also, reported by other researchers.[4,27,28] These IMCs are formed in the vicinity of the Al_7Cu_2Fe and Si-rich particles. In the presence of copper, copper is substituted into the crystal structure of the nickel aluminide structure.[29–31] Given the substitution of copper with nickel, the following equation may be suggested for the formation of Al_3NiC:

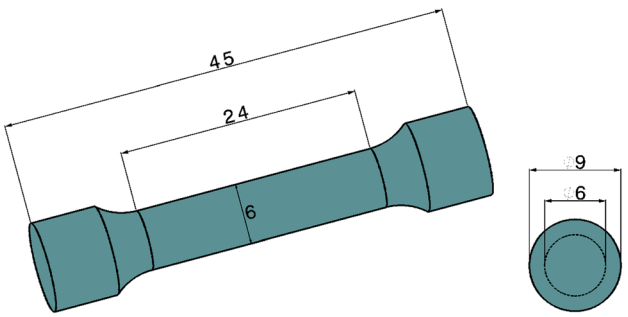

Figure 4. Tensile test sample dimensions (dimensions are in mm).

$$3Al + 2\ Ni \xrightarrow{\text{Cu substitution}} Al_3NiCu \qquad \text{Eqn. 2}$$

As can be seen, after homogenizing and aging treatment in the sample containing 1.5 wt% nickel, a continuous network of IMCs and second phase particles were formed at the boundary between the dendrites. It should be noted that with the addition of nickel up to 3 wt% as well as the aging process, S- Al_2CuMg precipitates will be reduced and their size will be smaller. However, after adding 4.5 wt% of nickel and also performing aging heat treatment, due to the absorption of large amounts of copper in the aluminum matrix by nickel-rich compounds, it is not possible to precipitate the S- Al_2CuMg precipitates, and, instead of it, the T-Al_6CuMg_4 precipitates will be formed. According to the reference,[32] the addition of nickel in the Al-Cu-Mg alloy system reduces the solubility of copper in the alloy and, due to the formation of Al-Ni-Cu intermetallic compounds (such as Al_3NiCu, Al_7NiCu_4), the ratio of copper to magnesium in the aluminum matrix is reduced. In this condition, the S- Al_2CuMg precipitation capability decreases. As can be seen, in the nickel-containing samples, after the aging heat treatment, the amount of Al_3NiCu compounds is reduced and the amount of Ni-Fe-rich compounds (Al_9NiFe) is increased.

Figure 9 shows the XRD results of different samples. By comparing XRD results reported in the ref.[19] as can be seen in the nickel-free sample (sample S-0), aging treatment does no effect on the nature of the particles and precipitates in the microstructure. Although Si-rich and Al (Cu, Mg, Si) particles were observed in the SEM microstructure, due to their small amounts, their peaks did not appear in the XRD results. By adding 1.5% nickel, no trace of nickel-rich IMCs is observed in the XRD results. Although these compounds were observed in the SEM microstructure, due

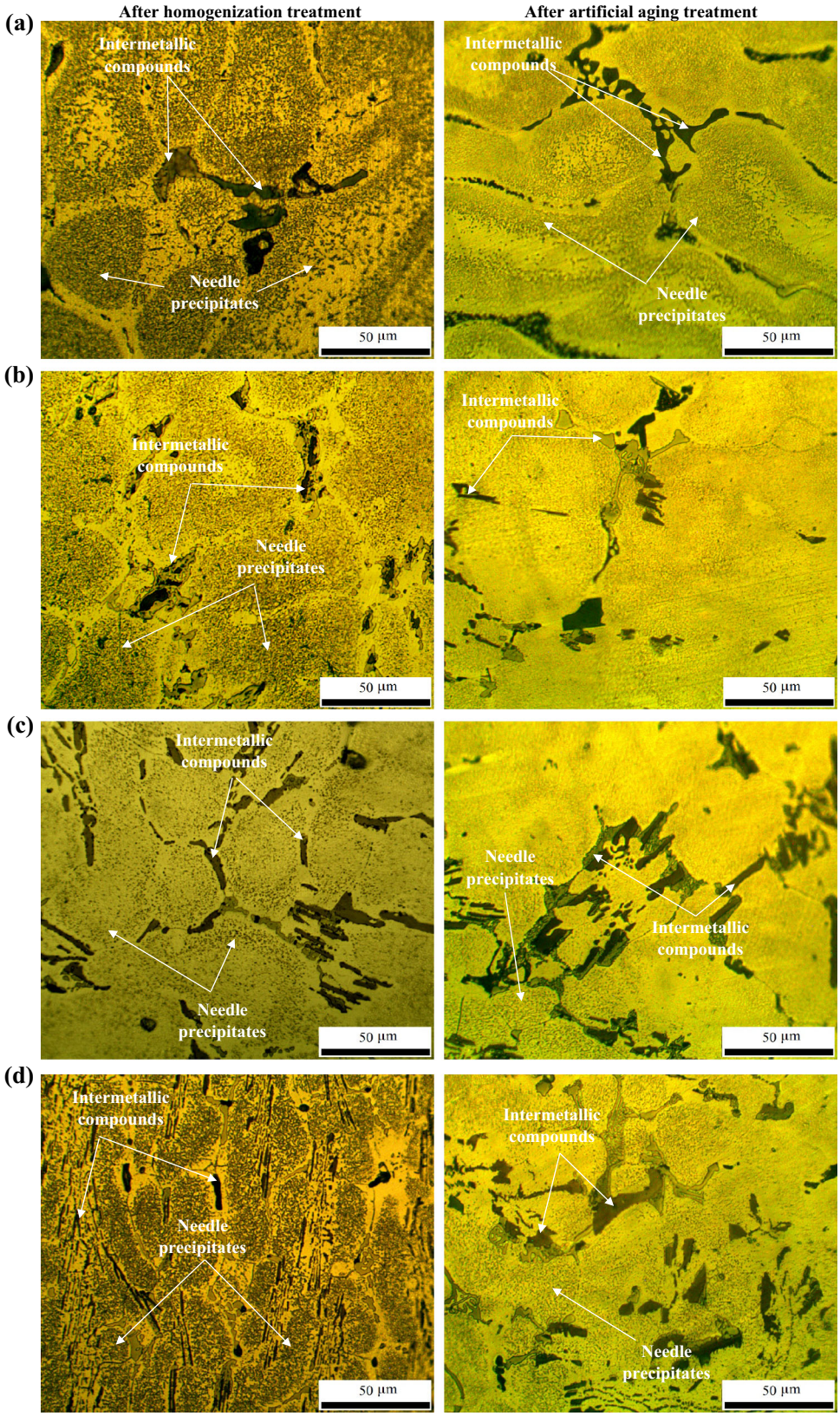

Figure 5. The optical microscopy images of; (a) sample S-0, (b) sample S-1.5, (c) sample S-3, (d) sample S-4.5.

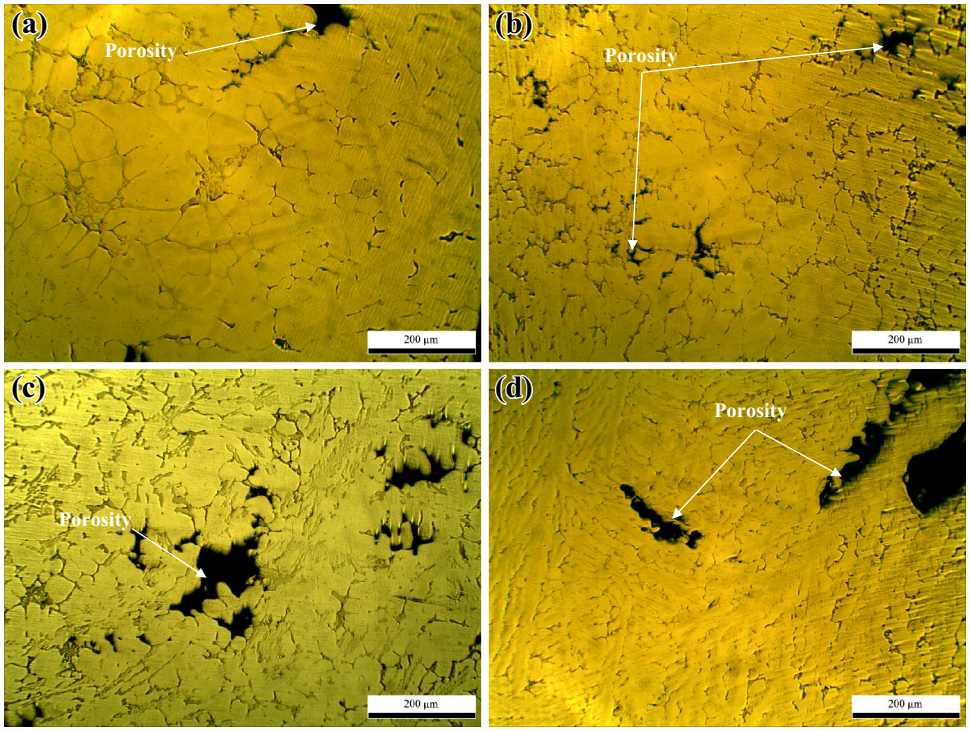

Figure 6. The optical microscopy image of porosity in; (a) sample S-0, (b) sample S-1.5, (c) sample S-3, (d) sample S-4.5.

to the small amount of these IMCs, they could not be detected using XRD results. With the addition of 3 wt% nickel, it is observed that in addition to S-Al_2CuMg and Al_7Cu_2Fe precipitates and particles, Al_3NiCu IMCs is also formed in the microstructure. In the homogenized 4.5 wt% nickel sample, it is observed that, similar to the sample S-3 sample, nickel-rich intermetallic is formed and the peak intensity of this compound increases. Another important point is that in both homogenized and aged samples S-4.5, the S-Al_2CuMg precipitates peak has been disappeared and the T-Al_6CuMg_4 precipitates peak has appeared. In all samples, compared to homogenized samples, the aging treatment has little effect on the nature of the precipitates. However, with the aging treatment and, also, adding nickel, the peak intensity of S-Al_2CuMg decreases. Based on the XRD results, quantitative analysis of S-Al_2CuMg, T-Al_6CuMg_4 and nickel-rich particles in different samples is shown in Figure 10. As can be seen, in the nickel-free sample, after aging treatment, the S-Al_2CuMg precipitate content increases, but in nickel-containing samples, the aging heat treatment reduces S-Al_2CuMg precipitates and increases the nickel rich particles amount.

Mechanical Properties

Variations in the hardness of different samples after homogenization and aging treatment are shown in Figure 11. As can be seen, the average hardness of the sample containing 3 wt% Ni, in both homogenized and aged states, is maximized and reached 144.05 and 134.10 HV, respectively. In all aged samples, except sample S-3, the hardness after aging increases, compared to the homogenized state. The formation of fine precipitates, IMCs with a lower aspect ratio, and a more uniform distribution of precipitates and particles in the microstructure can result in higher hardness after aging treatment. The formation of fine and uniform precipitates, and IMCs creates more strain fields and, due to the interaction of these strain fields with dislocation, the motion ability of dislocation is reduced, and, finally, the hardness as well as the strength of samples increase.[33] The lower hardness of artificially aged sample S-3, compared to homogenized sample S-3, can be attributed to the lower amount of the S-Al_2CuMg precipitates in the aged state. As the weight percentage of nickel increases, the amount of Al-Ni-based IMCs increases. Since these IMCs have high hardness,[4] it is expected that the formation of these IMCs is the main factor in increasing the hardness by adding nickel in these alloys. Similar results have been reported on the effect of Al-Ni-based IMCs (such as Al_3Ni, Al_3NiCu) on increasing the hardness of aluminum alloys.[4,34,35] By comparing the two samples S-0 and S-1.5, it is observed that the hardness, after homogenization in the sample S-0, is slightly higher than the sample S-1.5. It should be noted that although nickel-rich IMCs can be formed in the sample S-1.5, it should be noted that the higher porosity percentage in the sample S-1.5 (Figure 12) as well as a lower amount of S-Al_2CuMg precipitates, can overcome on strengthening effect of nickel-rich IMCs. As a result, there is no significant increase in hardness compared

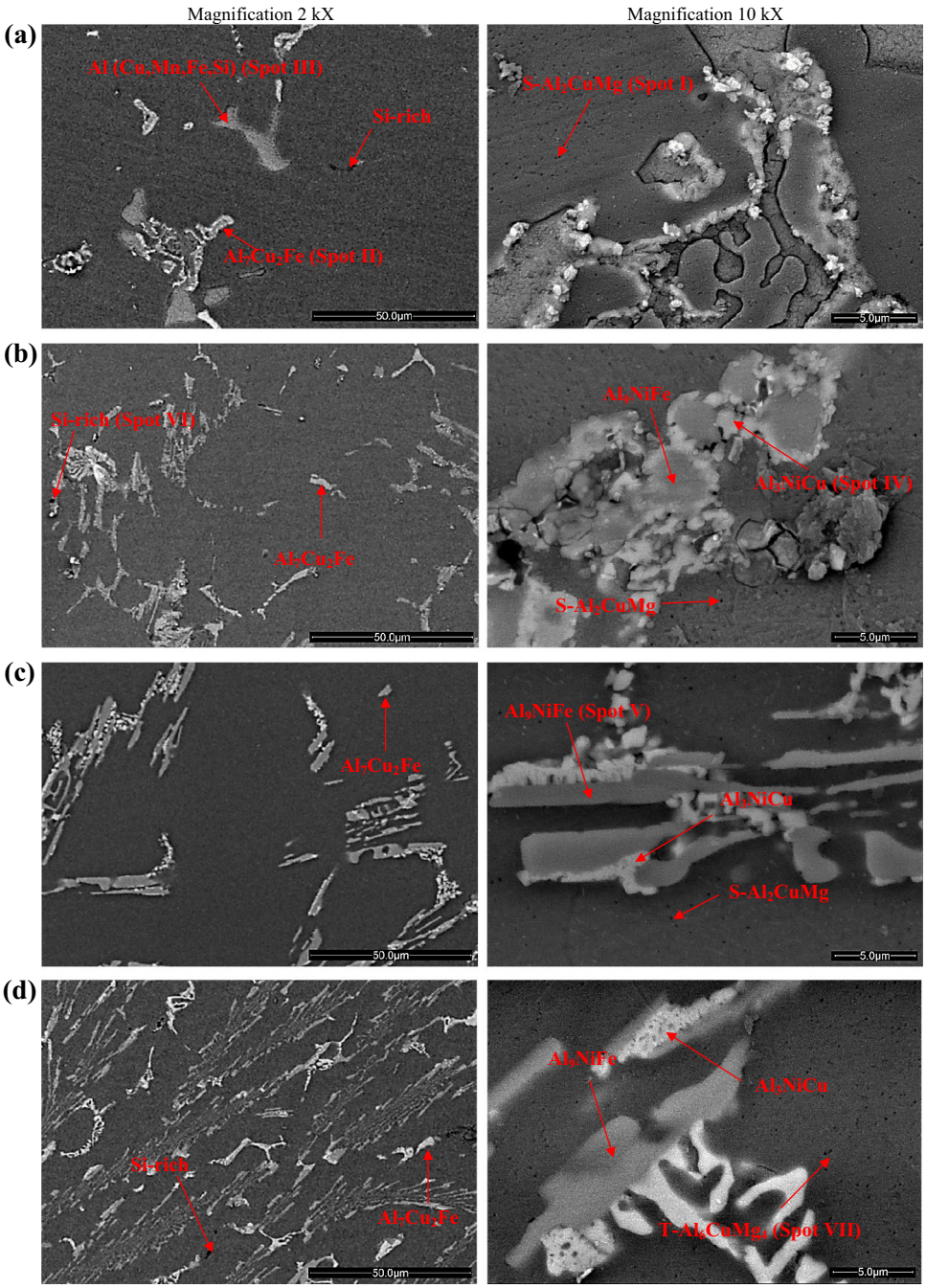

Figure 7. The SEM micrograph after aging treatment of; (a) sample S-0, (b) sample S-1.5, (c) sample S-3, (d) sample S-4.5.

to the sample S-0. With an increase in the percentage of nickel up to 3 wt%, it is observed that the hardness has increased significantly compared to the sample S-1.5. Although the presence of nickel in this sample can reduce S-Al_2CuMg precipitates, it is observed that the formation of a large amount of nickel-rich IMCs has led to a significant increase in hardness after homogenization. A further increase in the nickel content up to 4.5 wt% (sample S-4.5) reduced the hardness to 118.54 HV. Although more nickel-rich IMCs are formed in this sample, two factors can affect the reduction in hardness in this sample. First, formation of T-Al_6CuMg_4 precipitates in the aluminum matrix, and second, 44% increasing the porosity percent compared to the sample S-3. After aging heat treatment with increasing the percentage of nickel up to 3 wt%, the hardness has an upward trend, and this result is related to the formation of fine and uniform S-Al_2CuMg precipitates throughout the microstructure as well as the presence of nickel-rich IMCs. With increasing the percentage of nickel from 3 to 4.5 wt%, although there is a high percentage of nickel-rich IMCs in the microstructure, changing the nature of strengthening precipitates from S-Al_2CuMg to

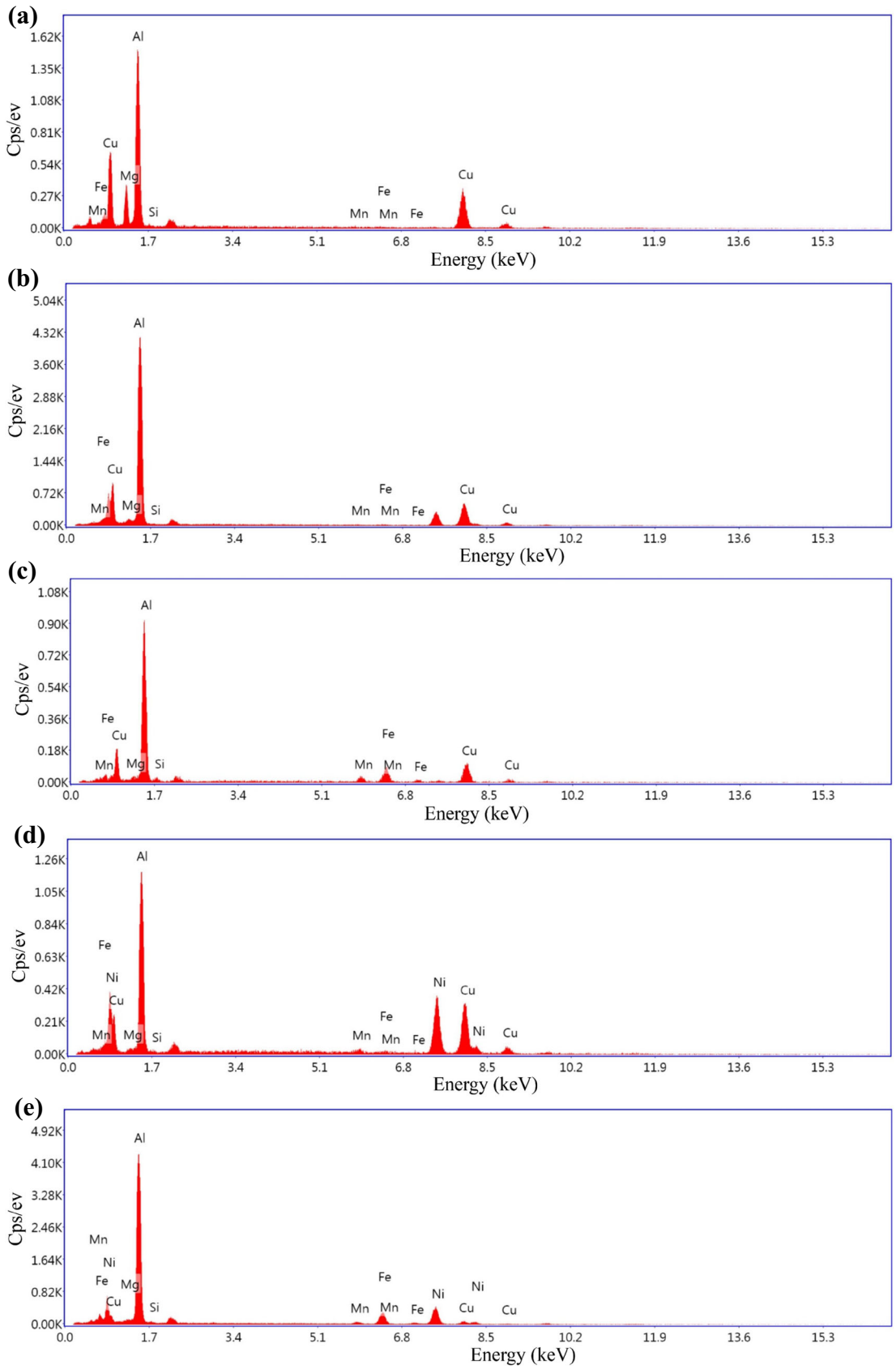

Figure 8. EDS analysis result of; (a) S-Al_2CuMg (spot I), (b) Al_7Cu_2Fe (spot II), (c) Al(Cu,Mn,Fe,Si) (spot III), (d) Al_3NiCu (spot IV), (e) Al_9NiFe (spot V), (f) Si-rich (spot VI), (g) T-Al_6CuMg_4 (Spot VII).

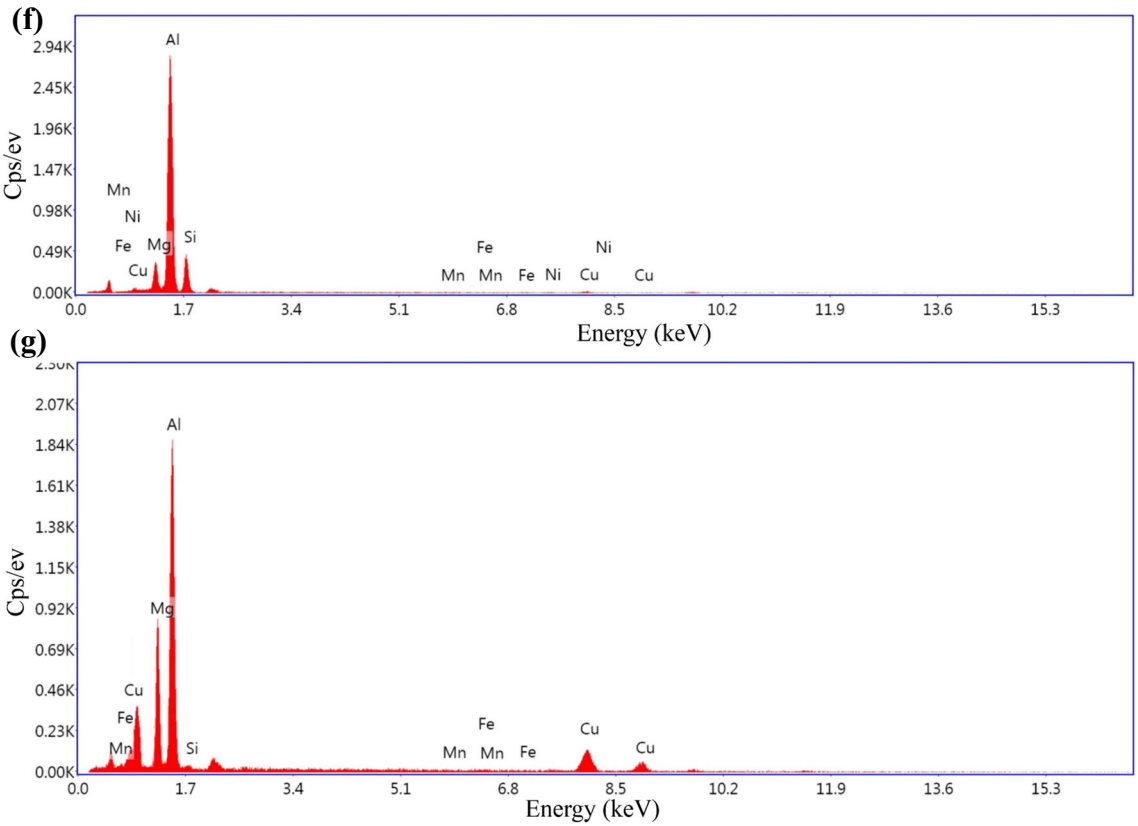

Figure 8. continued

T-Al_6CuMg_4, and also the presence of a high percentage of porosity again cause a decrease in hardness.

The results of the tensile test of different samples are presented in Figure 13 and Table 3. As can be seen, the ultimate tensile strength (UTS) of all aged samples increases concerning the homogenized state. The maximum UTS, after homogenization and aging treatment, was achieved in the sample S-3, as 251.23 and 230.76 MPa in both the aged and homogenized states, respectively. The

Table 2. EDS analysis result of S-Al_2CuMg (spot I), Al_7Cu_2Fe (spot II), Al(Cu,Mn,Fe,Si) (spot III), Al_3NiCu (spot IV), Al_9NiFe (spot V), Si-rich (spot VI), T-Al_6CuMg_4 (Spot VII).

Element	Fe	Mg	Cu	Ni	Si	Mn	Al
Spot I							
Atomic %	0.18	3.21	3.56	-	0.11	0.19	92.75
Spot II							
Atomic %	6.51	0.67	13.42	-	0.16	0.21	79.03
Spot III							
Atomic %	10.01	0.38	11.01	-	0.73	2.11	75.76
Spot IV							
Atomic %	0.85	0.88	14.69	15.23	0.56	0.71	67.08
Spot V							
Atomic %	17.45	0.56	0.95	16.02	0.78	0.93	63.31
Spot VI							
Atomic %	1.10	8.45	0.78	0.62	19.23	0.91	68.91
Spot VII							
Atomic %	0.93	27.11	4.15	-	0.34	0.78	66.69

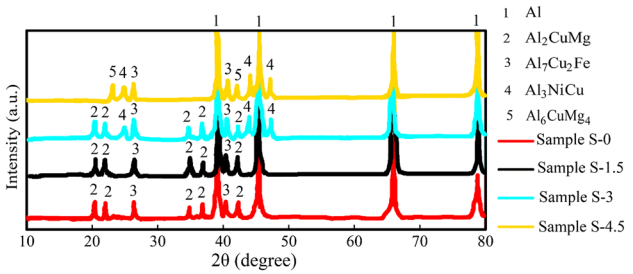

Figure 9. XRD pattern of different samples after aging heat treatment.

reason for the increase in the UTS after aging treatment of nickel-containing samples can be attributed to the presence of IMCs and fine strengthening precipitates in the microstructure. Also, after aging treatment, the IMCs in the inter-dendritic zone form a separate structure. In this case, the bond between the aluminum grains will be stronger, and, if microcracks are formed, it will not easily cause separation between the grains. The formation of interconnected IMCs at the grain boundary facilitates the nucleation and growth of microcracks in the microstructure. Variations in elongation and toughness of different samples are shown in Figures 13(c) and (d). As can be seen, the sample containing 3 wt% nickel present the greatest toughness and elongation. It is noteworthy that after aging treatment in all samples, strength and toughness increased and elongation decreased. The elongation in the sample S-3 in the aged and homogenized state is 1.52 and 1.60%, respectively, and the toughness in the aged and

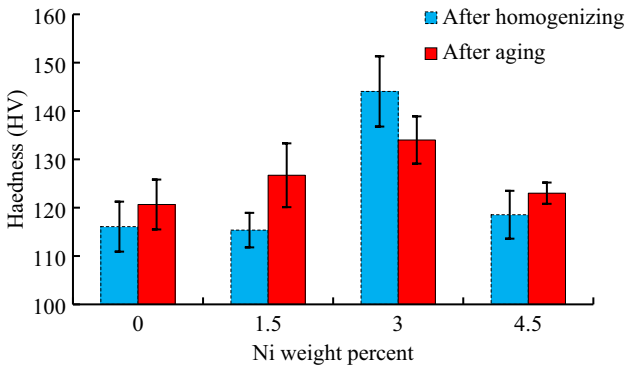

Figure 11. The average Vickers hardness of different samples.

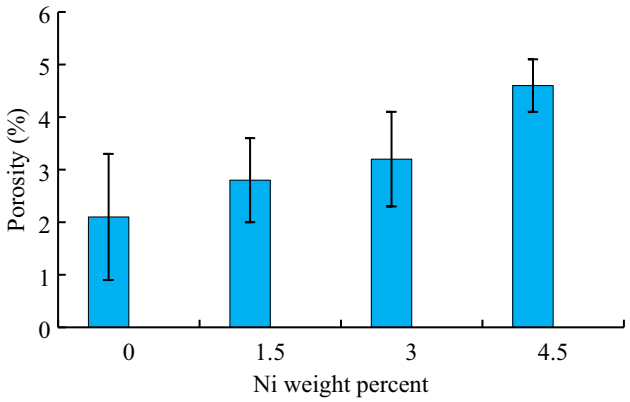

Figure 12. The porosity of different samples.

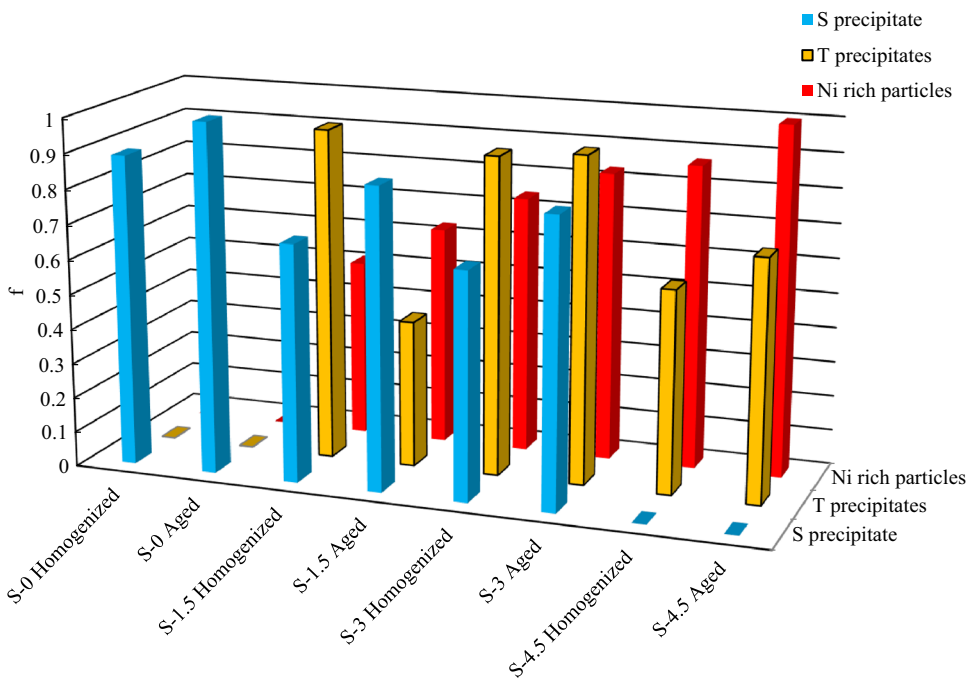

Figure 10. Quantitative analysis of S-Al_2CuMg, T-Al_6CuMg_4 and nickel-rich particles was performed in different samples ("Homogenized" means that the sample has been subjected to homogenization heat treatment and "Aged" means that artificial aging heat treatment was performed).

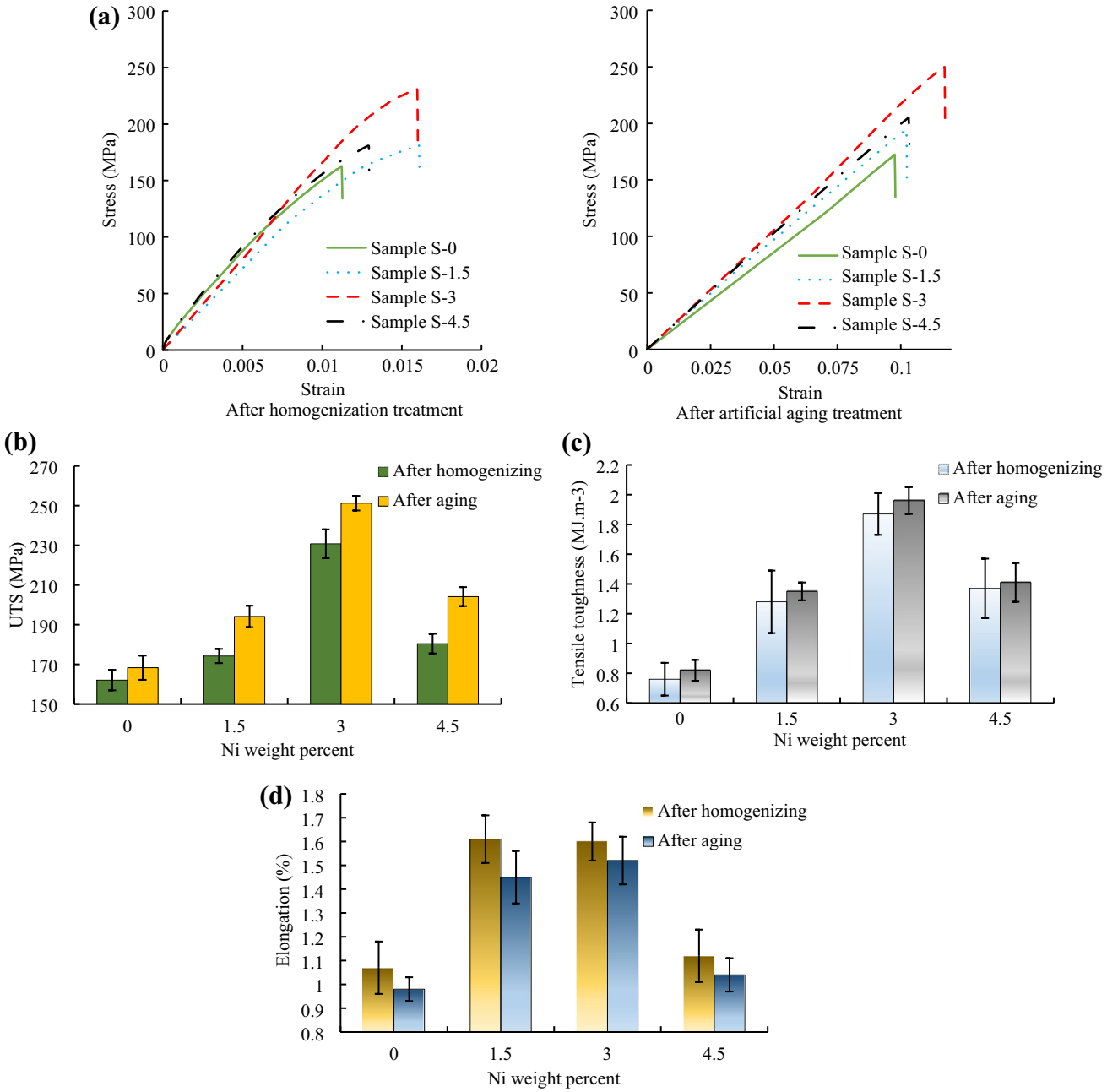

Figure 13. (a) tensile test curves, (b) ultimate tensile strength, (c) elongation, (d) tensile toughness of different samples.

Table 3. Mechanical properties of different samples

Sample no.	Yield strength (MPa)		Ultimate tensile strength (MPa)		Elongation (%)		Toughness (MJ.m^{-3})	
	HO*	Aged**	HO*	Aged**	HO*	Aged**	HO*	Aged**
S-0	140.1±2.2	152.7±3.4	162.0±5.1	168.3±6.1	1.07±0.11	0.98±0.05	0.76±0.11	0.82±0.07
S-1.5	151.6±3.1	180.8±2.7	174.2±3.5	194.1±5.4	1.61±0.10	1.45±0.11	1.28±0.21	1.35±0.06
S-3	202.4±2.7	230.6±4.1	230.7±7.2	251.2±3.7	1.60±0.08	1.52±0.10	1.87±0.14	1.96±0.09
S-4.5	162.4±3.4	190.5±2.8	180.4±4.9	204.1±4.8	1.12±0.11	1.04±0.07	1.37±0.20	1.41±0.13

*Homogenized sample

**Artificial aged sample

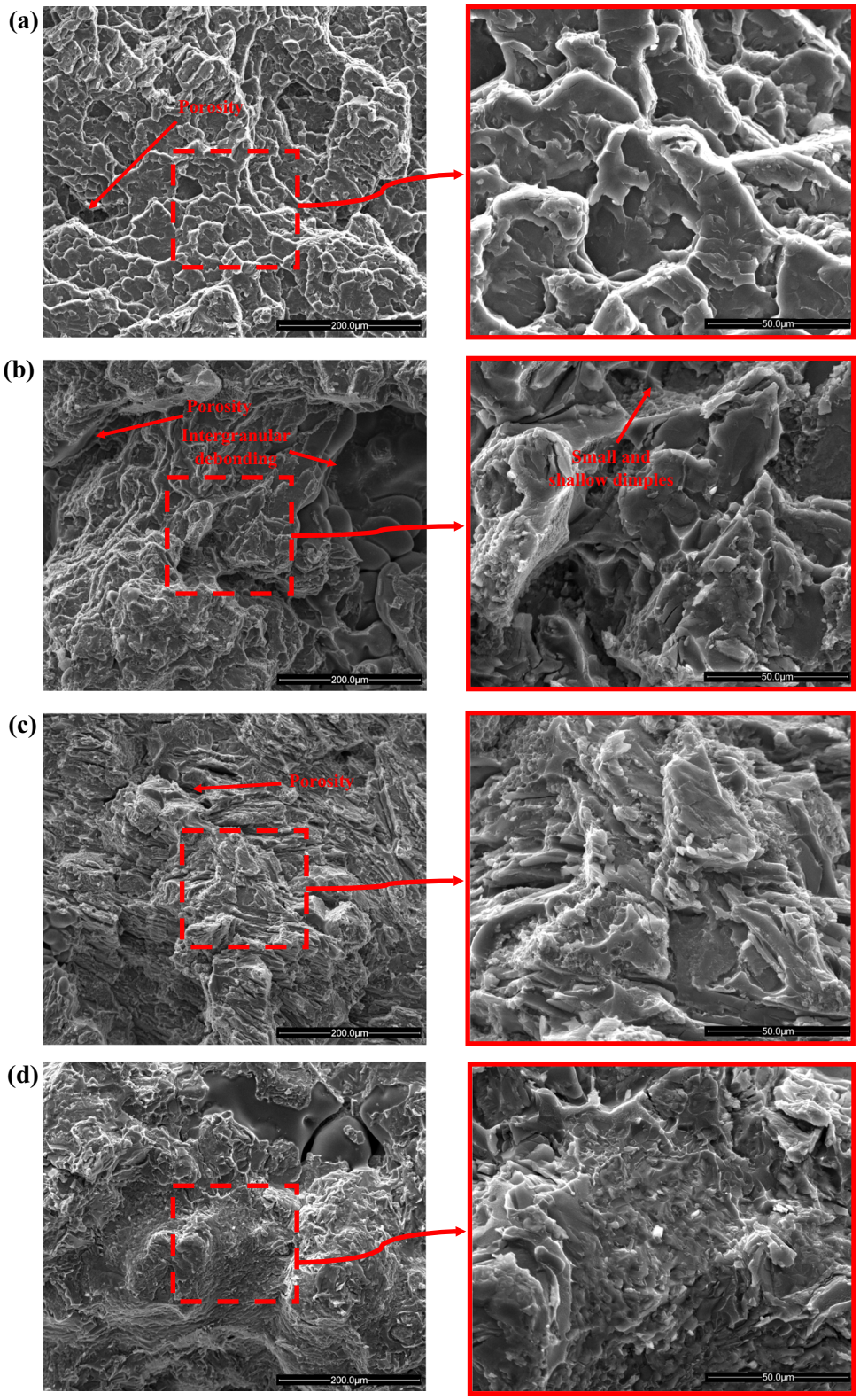

Figure 14. The SEM micrograph of fracture surface of; (a) sample S-0, (b) sample S-1.5, (c) sample S-3, (d) sample S-4.5.

homogenized state is equal to 1.96 and 1.87 $MJ.m^{-3}$, respectively. In sample S-4.5, the UTS, elongation, and toughness are reduced compared to sample S-3. The higher porosity (Figure 12) and the formation of T-Al_6CuMg_4 precipitates as well as IMCs with high aspect ratios can be the reason for the decrease in mechanical properties in this sample compared to sample S-3.

The Fracture surface of different samples after aging treatment is shown in Figure 14. The fracture behavior in all samples is mostly brittle. The cleavage fracture surface, fine cracks, shallow and fine dimples are observed on the fracture surface of all samples. By comparing results reported in the ref.[19] at the fracture surface of homogenized samples, a considerable amount of intergranular debonding is observed, the amount of which decreases with increasing the percentage of nickel as well as aging heat treatment. It is noteworthy that with the aging heat treatment, the ductile fracture feature at the fracture surface is significantly reduced. The intergranular debonding of aluminum indicates the presence of initial shrinkage porosity that exists between the aluminum grains. The eutectic melt in the microstructure can result in shrinkage porosity.[36] As the percentage of nickel increases, the amount of intergranular debonding of aluminum decreases due to the reduction of shrinkage porosity due to the eutectic structure. The reduction of shrinkage porosity, which means the reduction of eutectic structure, as reported by other researchers[37,38] can reduce the tendency to hot tearing. The fracture of nickel-rich particles and the lack of separation of the aluminum matrix from these particles indicate a very strong bond between these particles and the aluminum matrix. The presence of Fe-Ni-rich compounds with blade morphology can result in stress concentration and crack nucleation during the tensile test. Although after aging treatment the morphology of Fe-Ni rich compounds is somewhat changed from the blade shape, small amounts of these compounds in the microstructure act as crack nucleation sites. The presence of cracks in the cross-section of the samples S-3 and S-4.5 in the aged treated condition confirms that these IMCs with the blade morphology are one of the main reasons for strength reduction, especially in the sample S-4.5.

Conclusions

In this study, the effect of the nickel additive and artificial aging heat treatments on the microstructure and mechanical properties of the AA2024 aluminum alloy matrix composite reinforced with Al_3NiCu were investigated. The important findings of the study are as follows:

- After aging heat treatment in the nickel-free sample, the S-Al_2CuMg precipitates become finer and uniformly distributed throughout the microstructure. The inter-dendritic zone is also surrounded by Al_7Cu_2Fe and Al (Cu, Mn, Fe, Si) second phase particles.
- In the nickel-containing samples, after the aging heat treatment, the amount of Al_3NiCu intermetallic compounds is reduced and the amount of Ni-Fe rich compounds (Al_9NiFe) is increased.
- The formation of fine S-Al_2CuMg precipitates, intermetallic compounds with lower aspect ratios, and a more uniform distribution of precipitates and particles in the microstructure can result in higher mechanical properties after aging treatment.
- With increasing the percentage of nickel from 3 to 4.5 wt%, although there is a high percentage of nickel-rich intermetallic compounds in the microstructure, changing the nature of strengthening precipitates from S-Al_2CuMg to T-Al_6CuMg_4, and also the presence of a high percentage of porosity, causes a decrease in mechanical properties.
- The maximum hardness, ultimate tensile strength, and toughness after aging treatment achieved in the AA2024 aluminum alloy matrix composite containing 3 wt% nickel as 134.10 ± 4.89 HV, 251.23 ± 3.70 MPa, and 1.96 ± 0.09 $MJ.m^{-3,}$ respectively, due to the strengthening effect induced by intermetallic compounds and precipitates in the microstructure.
- The fracture behavior in all samples is mostly brittle. After aging heat treatment, the ductile fracture feature at the fracture surface is significantly reduced. Also, the presence of Fe-Ni-rich compounds with blade morphology can result in stress concentration and crack nucleation during the tensile test.

REFERENCES

1. I. Dinaharan, *Liquid metallurgy processing of intermetallic matrix composites, in: Intermetallic Matrix Composites*, Elsevier, 2018, pp. 167-202.
2. P. Ajay Kumar, P. Rohatgi, D. Weiss, 50 years of foundry-produced metal matrix composites and future opportunities. Int. J. Metalcast. **14**, 291–317 (2020). https://doi.org/10.1007/s40962-019-00375-4.
3. A. Gnanavelbabu, K.T.S. Surendran, S. Kumar, Process optimization and studies on mechanical characteristics of AA2014/Al_2O_3 nanocomposites fabricated through ultrasonication assisted stir–squeeze casting. Int. J. Metalcast. (2021). https://doi.org/10.1007/s40962-021-00634-3.
4. F. Liu, X. Zhu, S. Ji, Effects of Ni on the microstructure, hot tear and mechanical properties of Al–Zn–Mg–Cu alloys under as-cast condition. J. Alloys Compd. **821**, 153458 (2020)
5. R. Ramamoorthi, J.J.M. Hillary, R. Sundaramoorthy, J.D.J. Joseph, K. Kalidas, K. Manickaraj, Influence of stir casting route process parameters in fabrication of aluminium matrix composites–a review. Mater. Today Proc. **45**, 6660–6664 (2021)
6. P. Sahoo, S. Ghosh, Tribological behavior of aluminium metal matrix composites–a review. J. Tribol. Res. **2**, 1–14 (2011)

7. G.F. Aynalem, Processing methods and mechanical properties of aluminium matrix composites, Adv. Mater. Sci. Eng. 2020 (2020).
8. M.K. Sahu, R.K. Sahu, Fabrication of aluminum matrix composites by stir casting technique and stirring process parameters optimization, in: *Advanced Casting Technologies*, IntechOpen, 2018.
9. F. Badia, P. Rohatgi, *Dispersion of graphite particles in aluminum castings through injection of the melt* (1969).
10. V.M. Bermudez, Auger and electron energy-loss study of the Al/SiC interface. Appl. Phys. Lett. **42**, 70–72 (1983)
11. V.S. Ayar, M.P. Sutaria, Comparative evaluation of ex situ and in situ method of fabricating aluminum/TiB_2 composites. Int. J. Metalcast. **15**, 1047–1056 (2021). https://doi.org/10.1007/s40962-020-00539-7.
12. V.S. Ayar, M.P. Sutaria, Development and characterization of in situ $AlSi_5Cu_3$/TiB_2 composites. Int. J. Metalcast. **14**, 59–68 (2020). https://doi.org/10.1007/s40962-019-00328-x.
13. M. Zare, A. Maleki, B. Niroumand, In situ Al-SiOC composite fabricated by in situ pyrolysis of a silicone polymer gel in aluminum melt. Int. J. Metalcast. (2021). https://doi.org/10.1007/s40962-021-00658-9.
14. H. Demirtaş, R. Yildiz, E. Çevik, Mechanical and wear properties of high rate NiAl particle-reinforced Al composites produced by pressure infiltration method. Int. J. Metalcast. (2021). https://doi.org/10.1007/s40962-020-00564-6.
15. D. Yadav, R. Bauri, Nickel particle embedded aluminium matrix composite with high ductility. Mater. Lett. **64**, 664–667 (2010)
16. S. Arul, Effect of nickel reinforcement on micro hardness and wear resistance of aluminium alloy Al7075. Mater. Today: Proc. **24**, 1042–1051 (2020)
17. A. Sytschev, N. Kochetov, S. Vadchenko, D.Y. Kovalev, A. Shchukin, Processing of Ni–Al intermetallic with 2D carbon components. Mater. Chem. Phys. **238**, 121898 (2019)
18. M.T. Hayajneh, A.M. Hassan, Y.M. Jaradat, The effect of nickel addition, solution treatment temperature and time on the precipitation hardening of (Al-Cu) alloys. Acad. Edu **141**, 1–5 (2007)
19. R. Farajollahi, H. Jamshidi Aval, R. Jamaati, Effects of Ni on the microstructure, mechanical and tribological properties of AA2024-Al3NiCu composite fabricated by stir casting process. J. Alloys Compd. **887**, 161433 (2021)
20. A.R. Najarian, R. Emadi, M. Hamzeh, Fabrication of as-cast Al matrix composite reinforced by Al2O3/Al3Ni hybrid particles via in-situ reaction and evaluation of its mechanical properties. Mater. Sci. Eng., B **231**, 57–65 (2018)
21. R. Ramesh, S. Suresh Kumar, S. Gowrishankar, Production and characterization of aluminium metal matrix composite reinforced with Al3Ni by stir and squeeze casting, in: *Applied Mechanics and Materials*, Trans Tech Publ, 2015, pp. 315–319.
22. X. Zhang, H. Wang, C. Zou, Z. Wei, The evolution of microstructure and mechanical properties at elevated temperature of cast Al–Li–Cu–Mg alloys with Ni addition. J. Market. Res. **9**, 11069–11079 (2020)
23. M. Raei, M. Panjepour, M. Meratian, Effect of stirring speed and time on microstructure and mechanical properties of Cast Al–Ti–Zr–B 4 C composite produced by stir casting. Russ. J. Non-Ferrous Metals **57**, 347–360 (2016)
24. A. Handbook, Heat treating, vol. 4, ASM International, Materials Park, OH, 860 (1991).
25. S. Salarieh, S. Nourouzi, H. Jamshidi Aval, An investigation on the microstructure and mechanical properties of Al-Zn-Mg-Cu/Ti composite produced by compocasting. Int. J. Metalcast. (2021). https://doi.org/10.1007/s40962-021-00698-1.
26. R. Taylor, S. McClain, J. Berry, Uncertainty analysis of metal-casting porosity measurements using Archimedes' principle. Int. J. Cast Met. Res. **11**, 247–257 (1999)
27. A. Mohamed, F. Samuel, Microstructure, tensile properties and fracture behavior of high temperature Al–Si–Mg–Cu cast alloys. Mater. Sci. Eng., A **577**, 64–72 (2013)
28. M. Liang, L. Chen, G. Zhao, Y. Guo, Effects of solution treatment on the microstructure and mechanical properties of naturally aged EN AW 2024 Al alloy sheet. J. Alloys Compd. **824**, 153943 (2020)
29. S.-B. Yu, M.-S. Kim, Microstructure and high temperature deformation of extruded Al-12Si-3Cu-based alloy. Metals **6**, 32 (2016)
30. J.T. Kim, V. Soprunyuk, N. Chawake, Y.H. Zheng, F. Spieckermann, S.H. Hong, K.B. Kim, J. Eckert, Outstanding strengthening behavior and dynamic mechanical properties of in-situ Al–Al3Ni composites by Cu addition. Composites Part B Engineering **189**, 107891 (2020)
31. C. Chan, *Friction Stir Processing of Aluminium-Silicon Alloys*, The University of Manchester (United Kingdom), 2011.
32. L.F. Mondolfo, *Aluminum alloys: structure and properties* (Elsevier, Amsterdam, 2013)
33. G. Quan, L. Ren, M. Zhou, 2.13 Solutionizing and age hardening of aluminum alloys, in *Comprehensive Materials Finishing*. ed. by M.S.J. Hashmi (Elsevier, Oxford, 2017), pp. 372–397
34. Z. Gxowa-Penxa, P. Daswa, R. Modiba, M. Mathabathe, A. Bolokang, Development and characterization of Al–Al3Ni–Sn metal matrix composite. Mater. Chem. Phys. **259**, 124027 (2021)
35. P. Hernández, H. Dorantes, F. Hernández, R. Esquivel, D. Rivas, V. López, Synthesis and microstructural characterization of Al–Ni3Al composites fabricated by press-sintering and shock-compaction. Adv. Powder Technol. **25**, 255–260 (2014)

36. J.R. Davis, *Aluminum and aluminum alloys* (ASM International, Almere, 1993)
37. Y. Yoshida, H. Esaka, K. Shinozuka, Effect of solidified structure on hot tear in Al-Cu alloy, in: *IOP Conference Series: Materials Science and Engineering*, IOP Publishing, 2015, pp. 012059.
38. J.-Q. Han, J.-S. Wang, M.-S. Zhang, K.-M. Niu, Relationship between amounts of low-melting-point eutectics and hot tearing susceptibility of ternary Al–Cu– Mg alloys during solidification. Trans. Nonferrous Metals Soc. China **30**, 2311–2325 (2020)